



HOKKAIDO UNIVERSITY

Title	The Studies on the Relation between Pore Distribution of Volcanic Ejectas and Distance from Crater
Author(s)	TSUJINAKA, Nobuo; SASAKI, Tatsuo; MADAKA, Takashi et al.
Citation	Journal of the Faculty of Agriculture, Hokkaido University, 56(3), 267-291
Issue Date	1971-01
Doc URL	https://hdl.handle.net/2115/12852
Type	departmental bulletin paper
File Information	56(3)_p267-291.pdf



THE STUDIES ON THE RELATION BETWEEN PORE DISTRIBUTION OF VOLCANIC EJECTAS AND DISTANCE FROM CRATER

Nobuo TSUJINAKA, Tatsuo SASAKI,* Takashi MAEDA
and Seiichi SASAKI

(Department of Agricultural Engineering, Faculty of Agriculture,
Hokkaido University, Sapporo, Japan)

*(Department of Agricultural Chemistry, Hokkaido Agricultural
Experiment Station, Sapporo, Japan)

Received June 12, 1970

In some cases, a huge of pumiceous ejectas which are constructed by andesitic or dacitic materials were erupted from crater. Such an ejecta is made by principally pumice, plagioclase, pyroxene, or mixture of these minerals; occasionally, pumice block included such crystalline minerals. Generally if the erupted materials were young, these minerals are fresh and look like crystalline sandy matters. But these sands are different from general seashore- or river-sands in order to have the high water holding capacity;¹⁾ therefore these materials are special for the soil genetic process, and the soil derived from these materials shows some speciality on the crop cultivation.

The pyroclastic matters erupted from crater high above in the air are transported to the eastern side of the mountain in general by the prevailing westerly and are distributed over that direction. The mineral constituents and particle sizes are classified during the transportation,²⁾ and the particle size is smaller according to the length of the distances. The weathering process of smaller particles might go faster than the larger one, this phenomenon will be based on the high water holding capacity of smaller particle group from one reason; and one other, main reason is that the mineral constituents are more basic.

Surely, some determination methods of pore of soils were proposed.³⁾ But the authors have stated the determination method for pumice pores,⁴⁾ this time, in this report, they made an attempt to find, using the similar, and yet the improved method, relation between the pore distribution of pyroclastic materials and the distance from crater.

The authors thought that the smaller particles would have much pore space than the larger ones, so they collected samples according to distances

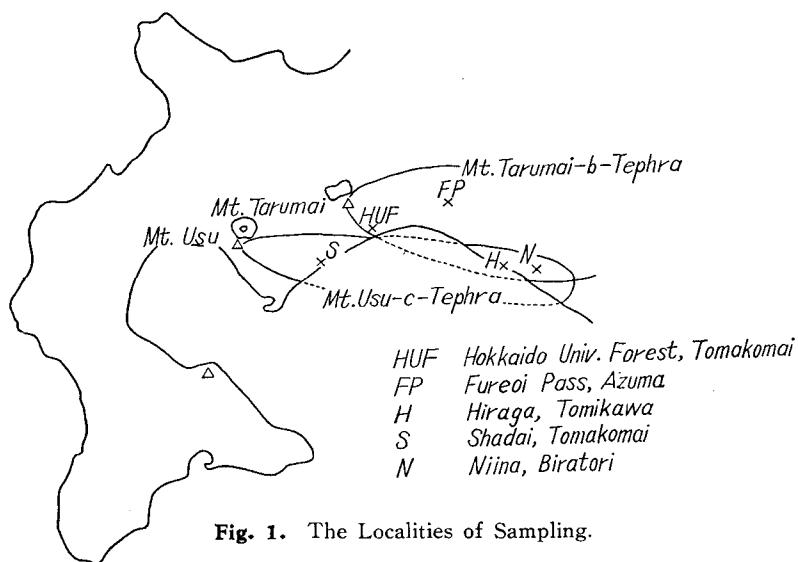


Fig. 1. The Localities of Sampling.

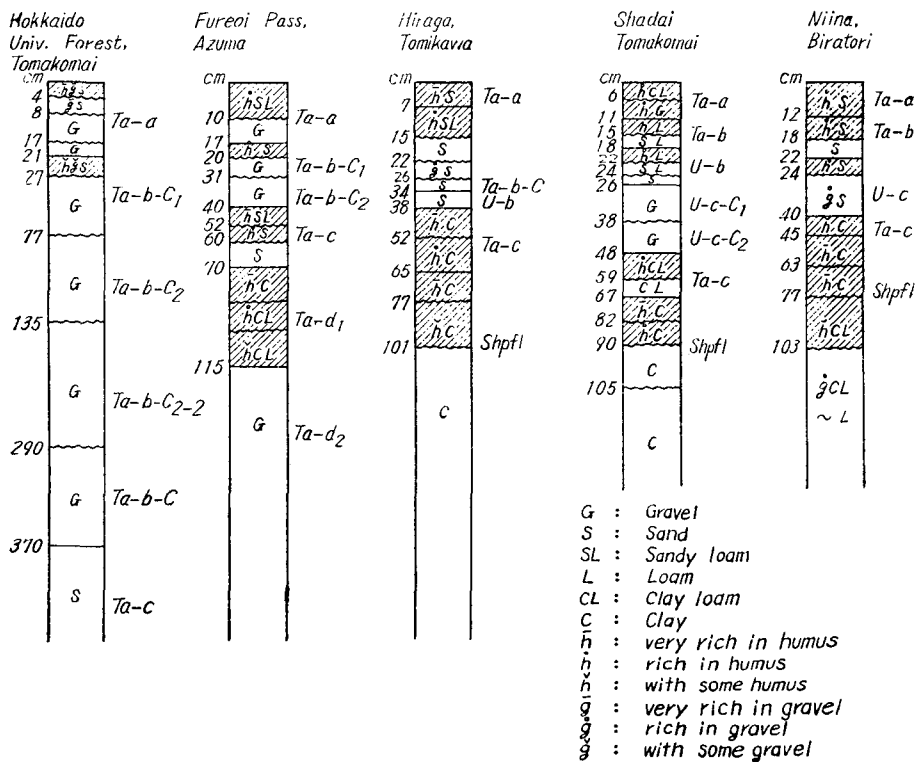


Fig. 2. Soil Profiles of Sampling Sites.

from the volcanos; these are Mt. Tarumai-b-Tephra layer at the Experimental Forest of Hokkaido University in Tomakomai City, Fureoi Pass in Azuma Village, and Hiraga in Tomikawa Town. The distances are 12, 43, and 61 km away from Mt. Tarumai respectively; and the others are Mt. Usu-c-Tephra layer at Shadai in Tomakomai C. and Niina in Biratori T. which are located respectively 48.5 and 64 km away from Mt. Usu.

But in this report, the authors would like to state Mt. Tarmai-b-Tephra samples principally by the reason from showing the similar inclination with the other samples which they are going to explain afterwards. The locations of samples were collected is shown in Fig. 1 and the soil profiles is in Fig. 2.

Samples

The samples were taken by stainless steel pipe (15 cm dia. \times 15 cm high) driven into each layer at the above-mentioned spots. The collected samples were air-dried and sieved by eight diameter sieves i.e. 0.25, 0.42, 0.84, 2.0, 4.8, 9.52, 19.1 and 25.4 mm and separated them into nine portions. Furthermore, the portions which are larger than 0.84 mm were separated into the groups, such as, pumice, lithic rock fragments (pale blue and reddish brown), and feldspar.

The particle size and mineralogical distributions are shown in Fig. 3 and Table 1. Middle diameter (Md), sorting grade (So), skewness (Sk), Kurtosis (K) are calculated from this particle-size summation curves (Fig. 3), and the data are shown in Table 2. Both the Md and the So show smaller values according to the distances from the volcanos, and this table shows that the diameter of particles has inclination to concentrate within a certain limited range in the farther distant areas from the volcanos.

Although the authors took Mt. Tarumai-b-Tephra samples at Hokkaido Univ. Forest, in Tomakomai, Fureoi Pass, in Azuma, and Hiraga in Tomikawa, it is possible to divide this Tephra into some layers and/or horizons by the grades of weathering, mineral constituents, colors, sizes and etc; four horizons C_1 , C_2 , C_{2-2} , C_3 , for Tomakomai, two horizons C_1 and C_2 for Azuma, and a layer C_1 for Tomikawa. And also they took Mt. Usu-c-Tephra at Shadai in Tomakomai and Niina in Biratori, and it divided into two horizons C_1 , C_2 for Shadai and a layer C_1 for Niina. However, it is very difficult to identify these layers and/or horizons respectively among each profile. Most of larger minerals are pumice, but the constituents of smaller particles tend to increase the including rate of lithic fragment and feldspar; especially, in the case of the particle size being smaller than 2 mm, the weight of pumice is lighter than the other crystalline minerals.

TABLE 1. Particle Size and Mineralogical Distribution of Tarumai-b-Tephra and Usu-c-Tephra. (Vl %)

Tephra	Locality	Horizon or Layer	Diameter mm. Pyroclastics	>25.4	25.4-19.1	19.1-9.52	9.52-4.8	4.8-2.0	2.0-0.84	0.84-0.42	0.42-0.25	<0.25
Tarumai-b-Tephra	Hokkaido Univ. Forest, Tomakomai	C ₁	Pumice B.L.F.* R.L.F.* Feldspars		0.23	5.75 0.59	9.52 2.39 0.10	14.51 8.12 0.27 0.28	9.55 20.29 0.06 6.28	19.53	1.33	1.20
		C ₂	Pumice B.L.F. R.L.F. Feldspars	1.72	3.36	11.18 0.12	16.99 0.83 0.74	18.88 1.81 2.00	10.39 11.90 1.82 3.03	11.81	1.51	1.87
		C ₂₋₂	Pumice B.L.F. R.L.F. Feldspars		2.62	20.16 0.08 0.11	20.65 0.64 0.51 0.10	12.11 7.27 0.92 0.76	5.03 14.28 0.70 5.05	7.42	1.12	0.47
		C ₃	Pumice B.L.F. R.L.F. Feldspars	4.87	5.81	40.11 0.60	21.76 1.16 0.91 0.04	3.07 7.79 0.89 0.54	1.23 5.37 0.06 0.97		3.42	0.81
	Fureoi Pass, Azume	C ₁	Pumice B.L.F. R.L.F. Feldspars			1.43	6.10 0.06	19.52 3.33 0.30 0.23	13.56 24.38 0.78 8.33	18.07	2.09	3.42
		C ₂	Pumice B.L.F. R.L.F. Feldspars		0.25	6.21	21.69 0.05 0.02	24.22 3.14 1.22 0.51	3.12 25.85 0.97 4.43	5.87	0.83	1.62
Hiraga	C	Pumice B.L.F. R.L.F. Feldspars				0.13	2.32 0.07 0.01	15.36 3.01 0.56 2.99	58.42	11.63	5.50	
Usu-c-Tephra	Shadai	C ₁	Pumice B.L.F. R.L.F. Feldspars		0.28	12.33	35.29	18.22 4.57 1.76 0.11	5.20 9.17 1.77 4.62	3.32	1.04	2.32
		C ₂	Pumice B.L.F. R.L.F. Feldspars			11.83	31.01	19.24 1.92 1.10 0.09	11.10 7.08 1.30 4.90	6.78	1.67	1.98
	Niina	C	Pumice B.L.F. R.L.F. Feldspars				0.13	16.15	53.64	22.88	4.10	3.10

TABLE 2. The Analysis of Particle Distribution

Tephra	Tarumai-b-Tephra							Usu-c-Tephra		
Locality	Tomakomai				Fureoi		Hiraga	Shadai		Niina
Horizon or Layer	C ₁	C ₂	C ₂₋₂	C ₃	C ₁	C ₂	C	C ₁	C ₂	C
Middle diameter (Md)	1.6	2.8	4.0	10.0	1.15	2.60	0.64	4.7	3.8	1.15
Sorting grade (So)	2.01	2.43	2.45	1.73	1.41	1.98	1.28	2.05	2.25	1.48
Skewness (Sk)	1.25	1.00	0.84	0.75	1.11	1.06	1.03	0.62	0.69	0.94
Kurtosis (K)	0.19	0.22	0.29	0.28	0.13	0.27	0.17	0.30	0.30	0.21

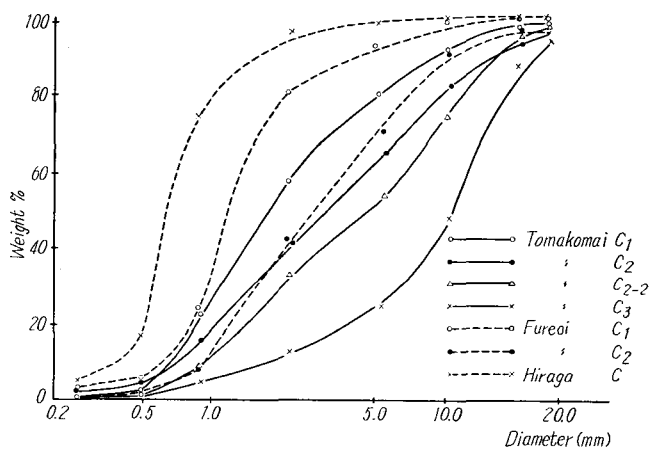


Fig. 3A. Particle Size Distribution of Tarumai-b-Tephra.

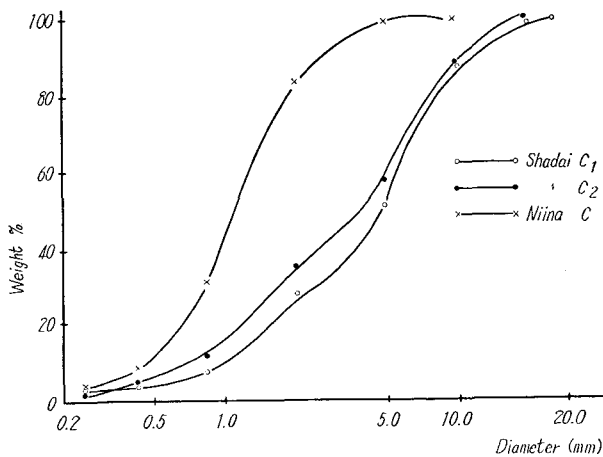


Fig. 3B. Particle Size Distribution of Usu-c-Tephra.

Classification and Determination of Pores of Pumice and Pyroclastic Materials

The authors classified the pores of pyroclastic materials as the following five types: These are (1) dead pore, (2) active pore, (3) semi-active pore, (4) secondary active pore, and (5) semi-dead pore.

The dead pore is a sealed pore in particles and has no passage to the surface, the active pore is a pore having an opening to the surface and water is admitted into there easily; the semi-active pore is also a pore at the surface, or is present in the active pore, but admission of water is restricted to some extent because of the narrower diameter than the active pore; the secondary active pore is a kind of the dead pore but isolated from the surface, or the active- or semi-active- pores with thin membranes which will be broken by small positive or negative pressure; and the semi-dead pore is a pore having a very narrow passage to the surface and it is too narrow to pass water in liquid but it is possible for vapor only.

The determination method for these five-type pores is as follows:

(I) The authors determined the specific gravity (H) of each separated sample with Beckmann's air comparison pycnometer.

(II) After H were determined the samples were transported into wide-mouth glass pycnometers and sank them in water at room temperature and stood them still in ordinal pressure for 24 hrs. and determined specific gravity (D) by routine method.

(III) After determination of D, the sample sunk in water was vacuumed in 0.002 mm Hg for 4 hrs. and determined specific gravity (F).

(IV) Samples after determined F were dried in air oven (105°C) and decided the weight, and it was used for the basis of calculations.

(V) After dried, the specific gravity (J) was determined by air comparison pycnometer.

(VI) Samples were paraffined, and then specific gravity (A) was determined.

(VII) Each sample was pulverized in mortar and specific gravity (B) was determined.

By these data the authors calculated the volume of each item as follows:

(I) The apparent solid phase from paraffine coated particles = 100

(II) The real solid phase $C = 100 A/B$

(III) The total pore $a = 100 - C$

(IV) The active pore $b = 100 (1 - A/D)$

(V) The secondary active pore $c = 100 A (1/H - 1/J)$

(VI) The semi-active pore $d = 100 A (1/D - 1/F) - c$

- (VII) The dead pore $e = 100 A/J - C$
- (VIII) The semi-dead pore $f = 100 A (1/F - 1/J)$

**The Solid Phase and the Pore of Pumice
and of Lithic Fragment**

The distribution of pores in the samples is shown in Table 3A-3J; The total pores of each pumice are increased according to the distances from volcanos, and such an inclination may occur by the classification of size or species of pumice by ejection and through flying, in this case the apparent gravity of pumice becomes smaller by increase of the pore volume and the pumice may be able to fly for longer distances, for instance, the apparent gravity of the 4.8-9.52 mm size pumices from Hokkaido Univ. Forest-C₁, Fureoi-C₁, and Hiraga samples are 1.61, 1.05, and 0.69; for Tarumai-b-Taphra they show 0.74 and 0.57 in Shadai-C₁ and Niina samples respectively.

The active pore volume is large in pumice which presents in longer distance from the mountain as well as the total pore volume, and at the same time, the larger pumice than 0.84 mm and having a large total pore volume is large in the active pore volume. The dead pore volume looks independent from the distance and the volume is about 5% average, but the range is from about 10% value to the one too small to determine for Tarumai-b-Tephra and 12.5-9.8% for Usu-c-Tephra. The content of the semi-dead pore becomes more abundant at the nearer place to the volcano and it reaches about 10-20% of the apparent solid phase, especially it is remarkable in Tomakomai-C₂ and -C_{2.2} pumices. The content of the semi-active pore shows the similar inclination to that of the active pore.

Generally speaking the pumice particles larger than 2 mm have larger volume of pore than the real solid phase volume and this ratio is higher in larger pumice, but for the smaller size particle, for instance, 0.84-2.0 mm, this inclination becomes reverse, i.e. the particle becomes smaller while the apparent gravity becomes larger. This phenomenon will be estimated that the pumices are classified while in flying.

The ratio of the active pore volume to the total pore volumes has a tendency to become higher to decreasing the size of pumice. On the other hand, the volume of the other type pores is getting smaller to the size of particles: this is remarkable in the semi-active and the semi-dead pores, and the system of the pore becomes simple to decreasing the size of particles.

For the lithic fragments, the volume of real solid phase is larger than that of pumice, even though the distances from the crater are short or long. The ratio of the volume of the real solid phase to the volume of the pore

TABLE 3-A. Pore Distribution of Tarumai-b-Tephra-C₁
at Tomakomai. (VI %)

Particle size mm.	Pyroclastic material	Apparent S. G.	S. G.	Solid phase	Total pore	Active pore	Semi-active pore	Dead pore	Semi-dead pore	Secondary pore
19.1 -25.4	Pumice	1.45	2.63	55.13	44.87	18.08	16.99	4.30	5.01	0.49
9.52-19.1	Pumice B.L.Fr.*	1.31	2.64	49.62	50.38	15.48	19.53	5.43	9.48	0.46
		2.16	2.86	75.52	24.48	1.37	10.47	6.61	6.03	—
4.8 -9.52	Pumice B.L.Fr. R.L.Fr.*	1.61	2.63	61.22	38.78	6.40	20.08	5.58	6.72	—
		2.13	2.78	81.92	18.08	5.75	9.39	2.30	0.64	—
		2.31	2.75	77.45	22.55	8.69	10.44	3.40	2.02	—
2.0 -4.8	Pumice B.L.Fr. R.L.Fr. Feldspars	1.60	2.66	60.15	39.85	14.44	16.91	5.69	2.54	0.27
		2.17	2.81	77.22	22.78	10.33	7.47	4.36	0.31	0.31
		2.10	2.84	76.64	23.36	18.60	1.25	2.91	0.60	—
		2.21	2.74	80.66	19.34	14.34	3.20	1.80	—	—
0.84-2.0	Pumice B.L.Fr. R.L.Fr. Feldspars	1.53	2.49	61.45	38.55	24.63	11.12	0.75	0.76	1.29
		2.41	3.04	79.28	20.72	13.31	4.44	—	2.87	—
		—	—	—	—	—	—	—	—	—
		2.25	2.69	83.64	16.36	12.11	2.34	1.59	0.32	—
0.42-0.84	mixture		2.95							
0.25-0.42	mixture		3.21							
<0.25	mixture		2.65							

* B.L.Fr.: Blue Lithic Fragment

* R.L.Fr.: Red Lithic Fragment

TABLE 3-B. Pore Distribution of Tarumai-b-Tephra-C₂
at Tomakomai. (VI %)

Particle size mm	Pyroclastic material	Apparent S.G.	S.G.	Solid phase	Total pore	Active pore	Semi-active pore	Dead pore	Semi-dead pore	Secondary pore
>25.4	Pumice	1.24	2.62	47.33	52.63	13.89	19.80	5.66	13.32	—
19.1 -25.4	Pumice	1.01	2.58	39.15	60.85	13.68	14.92	5.15	26.33	0.77
9.52-19.1	Pumice	1.28	2.61	49.04	50.96	5.19	19.55	8.62	16.33	1.27
4.8 -9.52	Pumice	1.10	2.63	41.83	58.17	17.71	17.78	7.06	12.56	1.06
	B.L.Fr	2.44	2.74	89.05	10.95	5.06	4.90	0.99	—	—
	R.L.Fr	2.45	2.74	89.42	10.58	3.54	4.01	3.03	—	—
2.0 -4.8	Pumice	1.20	2.64	45.45	54.55	28.57	13.75	6.00	5.10	1.08
	B.L.Fr	2.64	3.21	82.24	17.76	7.37	0.32	6.35	3.72	—
	R.L.Fr	2.36	2.75	85.82	14.18	8.89	2.72	2.57	—	—
0.84-2.0	Pumice	1.33	2.64	50.38	49.62	37.56	3.06	4.58	4.42	—
	B.L.Fr	2.86	3.21	89.10	10.92	9.21	1.13	0.58	—	—
	R.L.Fr	—	2.67	—	—	—	—	—	—	—
	Feldspars	—	—	—	—	—	—	—	—	—
0.42-0.84	mixture		3.12							
0.25-0.42	mixture		2.81							
<0.25	mixture		2.64							

TABLE 3-C Pore Distribution of Tarumai-b-Tephra-C_{2,2}
at Tomakomai. (Vl %)

Particle size mm	Pyroclastic material	Apparent S.G.	S.G.	Solid phase	Total pore	Active pore	Semi-active pore	Dead pore	Semi-dead pore	Secondary pore
19.1 -25.4	Pumice	0.82	2.62	31.30	68.70	21.15	21.42	6.66	16.93	1.27
9.52-19.1	Pumice	0.90	2.62	34.35	65.65	19.64	22.91	4.28	15.72	1.55
4.8 -9.52	Pumice	1.08	2.65	40.75	59.25	19.40	13.86	9.95	15.08	0.48
	B.L.Fr.	2.40	2.70	88.89	11.10	2.44	6.99	1.68	—	—
	R.L.Fr.	2.44	2.74	89.05	10.95	6.87	1.82	2.26	—	—
2.0 -4.8	Pumice	1.19	2.74	43.43	56.57	27.23	12.34	8.73	11.79	0.48
	B.L.Fr.	2.70	3.14	85.99	14.01	8.00	5.73	—	—	0.28
	R.L.Fr.	2.43	2.75	88.36	11.64	10.66	—	0.98	—	—
	Feldspars	2.33	2.81	82.92	17.08	4.12	0.78	12.18	—	—
0.84-2.0	Pumice	1.55	2.66	58.27	41.73	23.27	8.75	1.12	8.59	—
	B.L.Fr.	3.03	3.27	92.94	7.06	6.50	0.56	—	—	—
	R.L.Fr.	2.35	—	—	—	—	—	—	—	—
	Feldspars	2.51	—	—	—	—	—	—	—	—
0.42-0.84	mixture		3.02							
0.25-0.42	mixture		2.96							
<0.25	mixture		2.63							

TABLE 3-D. Pore Distribution of Tarumai-b-Tephra-C₃
at Tomakomai. (VI %)

Particle size mm.	Pyroclastic material	Apparent S.G.	S.G.	Solid phase	Total pore	Active pore	Semi-active pore	Dead pore	Semi-dead pore	Secondary pore
>25.4	Pumice	0.70	2.62	26.72	73.28	22.22	40.15	5.99	4.92	—
19.1 -25.4	Pumice	0.93	2.62	35.50	64.50	18.42	33.64	4.93	7.51	—
9.52-19.1	Pumice	1.02	2.62	38.93	61.07	17.74	29.94	4.47	8.38	—
	B.L.Fr.	2.37	2.62	90.46	9.54	3.66	5.88	—	—	—
4.8 -9.52	Pumice	1.06	2.61	40.61	59.39	23.74	19.14	6.92	8.55	0.54
	B.L.Fr.	2.35	2.76	85.14	14.86	12.74	2.12	—	—	—
	R.L.Fr.	2.20	2.69	81.78	18.22	15.08	3.14	—	—	—
2.0 -4.8	Pumice	1.35	2.70	50.00	50.00	28.95	13.70	5.10	1.15	1.04
	B.L.Fr.	2.53	3.02	83.77	16.23	10.92	1.84	1.63	1.84	—
	R.L.Fr.	2.37	2.69	88.10	11.90	7.62	4.78	—	—	—
	Feldspars	2.37	2.75	86.18	13.82	11.62	2.20	—	—	—
0.84-2.0	Pumice	1.56	2.62	59.54	40.46	27.35	0.53	—	1.40	1.10
	B.L.Fr.	2.94	3.18	92.42	7.55	7.02	0.53	—	—	—
	R.L.Fr.	—	—	—	—	—	—	—	—	—
	Feldspars	—	—	—	—	—	—	—	—	—
0.42-0.84	mixture		2.79							
0.25-0.42	mixture		2.93							
<0.25	mixture		2.62							

TABLE 3-E. Pore Distribution of Tarumai-b-Tephra-C₁
at Fureoi, Azuma. (VI %)

Particle size mm.	Pyroclastic material	Apparent S.G.	S.G.	Solid phase	Total pore	Active pore	Semi-active pore	Dead pore	Semi-dead pore	Secondary pore
9.52-19.1	Pumice	0.85	2.65	32.08	67.82	26.72	28.84	5.53	6.66	0.17
4.8 -9.52	Pumice	1.05	2.63	39.92	60.08	30.92	22.84	4.76	1.37	0.19
	B.L.Fr.	1.97	2.70	72.96	27.04	24.23	2.81	—	—	—
2.0 -4.8	Pumice	1.17	2.63	44.49	55.51	30.36	14.45	4.46	6.24	—
	B.L.Fr.	1.91	2.73	69.96	30.04	21.70	3.44	1.21	3.09	—
	R.L.Fr.	1.98	2.78	71.22	28.78	22.05	2.09	1.56	3.07	—
	Feldspars	2.44	2.70	90.37	9.63	8.96	—	0.67	—	—
0.84-2.0	Pumice	1.64	2.68	61.19	38.81	28.07	5.80	2.13	2.81	—
	B.L.Fr.	2.58	3.16	81.65	18.35	15.13	0.56	1.31	1.35	—
	R.L.Fr.	—	—	—	—	—	—	—	—	—
	Feldspars	2.37	2.70	87.78	12.32	11.57	0.33	0.32	—	—
0.42-0.84	mixture		3.00							
0.25-0.42	mixture		2.99							
<0.25	mixture		2.62							

TABLE 3-F. Pore Distribution of Tarumai-b-Tephra C₂
at Fureoi, Azuma. (Vl %)

Particle size mm.	Pyroclastic material	Apparent S.G.	S.G.	Solid phase	Total pore	Active pore	Semi-active pore	Dead pore	Semi-dead pore	Secondary pore
19.1 -25.4	Pumice	0.90	2.61	34.48	65.52	24.78	24.58	3.66	1.86	0.64
9.52-19.1	Pumice	0.99	2.62	27.79	62.21	18.18	32.28	4.16	7.06	0.53
4.8 -9.52	Pumice	0.97	2.60	37.31	62.69	29.71	25.28	3.62	0.57	0.51
	B.L.Fr.	1.86	2.69	69.14	30.86	28.19	2.41	0.26	—	—
2.0 -4.8	Pumice	1.07	2.59	41.31	58.69	31.85	18.61	3.84	4.39	—
	B.L.Fr.	2.56	2.96	86.49	13.51	11.14	2.37	—	—	—
	R.L.Fr.	2.17	2.77	80.37	19.63	17.18	2.15	0.30	—	—
	Feldspars	2.49	2.69	92.57	3.43	7.11	0.32	—	—	—
0.84-2.0	Pumice	1.92	2.79	68.82	36.18	20.99	6.56	1.51	2.12	—
	B.L.Fr.	2.98	3.30	90.30	9.70	7.74	0.85	1.11	—	—
	R.L.Fr.	2.15	2.70	79.63	20.37	20.07	—	0.30	—	—
	Feldspars	2.54	2.69	94.42	5.58	5.24	0.34	—	—	—
0.42-0.84	mixture		3.31							
0.25-0.42	mixture		3.17							
<0.25	mixture		2.69							

TABLE 3-G. Pore Distribution of Tarumai-b-Tephra C
at Hiraga, Tomikawa. (Vl%)

Particle size mm.	Pyroclastic material	Apparent S. G.	S. G.	Solid phase	Total pore	Active pore	Semi-active pore	Dead pore	Semi-dead pore	Secocdary pore
4.8 -9.52	Pumice	0.69	2.55	27.06	72.24	33.65	34.70	2.05	1.83	0.71
2.0 -4.8	Pumice B.L.Fr.	0.99 2.01	2.55 —	38.82 —	61.18 —	36.13 —	16.57 —	4.99 —	3.31 —	0.38 —
0.84-2.0	Pumice B.L.Fr. R.L.Fr. Feldspars	1.26 2.43 1.75 2.63	2.58 — — —	48.84 — — —	51.16 — — —	28.41 — — —	15.11 — — —	5.01 — — —	2.40 — — —	0.23 — — —
0.42-0.84	mixture		2.90							
0.25-0.42	mixture		3.01							
<0.25	mixture		2.74							

TABLE 3-H. Pore Distribution of Usu-c-Tephre C₁
at Shadai, Tomakomai. (Vl %)

Particle size mm.	Pyroclastic material	Apparent S. G.	S. G.	Solid phase	Total pore	Active pore	Semi-active pore	Dead pore	Semi-dead pore	Secondary pore
19.1 -25.4	Pumice	0.57	2.32	24.57	75.43	17.39	20.42	12.20	25.19	0.23
9.52-19.1	Pumice	0.66	2.32	28.45	71.55	13.16	32.29	10.60	15.05	0.45
4.8 -9.52	Pumice	0.74	2.33	21.76	68.24	8.64	31.42	12.55	15.37	0.26
2.0 -4.8	Pumice	0.79	2.32	34.05	65.95	15.05	26.59	11.88	12.16	0.27
	B.L.Fr.	2.18	2.66	81.95	18.05	12.40	1.97	2.22	1.46	—
	R.L.Fr.	2.28	2.69	84.76	15.24	13.96	0.65	0.63	—	—
0.84-2.0	Pumice	0.78	2.35	33.19	66.81	35.00	14.57	11.38	5.11	0.75
	B.L.Fr.	2.46	2.78	88.49	11.51	9.89	1.62	—	—	—
	R.L.Fr.	2.32	2.70	85.93	14.07	11.95	2.12	—	—	—
	Feldspars	2.45	2.67	91.76	8.24	8.24	—	—	—	—
0.42-0.84	mixture		2.60							
0.25-0.42	mixture		2.75							
<0.25	mixture		2.57							

TABLE 3-I Pore Distribution of Usu-c-Tephra C
at Shadai, Tomakomai. (VI %)

Particle size mm.	Pyroclastic material	Apparent S.G.	S.G.	Solid phase	Total pore	Active pore	Semi-active pore	Dead pore	Semi-dead pore	Secondary pore
9.52-19.1	Pumice	0.60	2.34	25.64	74.36	21.05	20.81	11.40	20.65	0.45
4.8 -9.52	Pumice	0.61	2.33	26.18	73.82	25.61	27.57	12.43	7.25	0.96
2.0 -4.8	Pumice	0.62	2.32	26.72	73.28	28.74	19.80	11.08	13.44	0.22
	B.L.Fr.	2.09	2.67	78.28	21.72	13.99	3.07	1.49	3.17	—
	R.L.Fr.	2.15	2.79	77.06	22.94	18.87	0.61	2.18	9.20	—
0.84-2.0	Pumice	0.66	2.33	28.33	71.67	38.89	18.30	10.27	3.98	0.23
	B.L.Fr.	2.44	2.75	88.73	11.27	10.29	0.98	—	—	—
	R.L.Fr.	2.46	2.65	92.83	7.17	6.15	1.02	—	—	—
	Feldspars	2.54	2.63	—	—	—	—	—	—	—
0.42-0.84	mixture		2.51							
0.25-0.42	mixture		2.70							
<0.25	mixture		2.47							

TABLE 3-J. Pore Distribution of Usu-c-Tephra C
at Niina, Biratori. (VI %)

Particle size mm.	Pyroczastic material	Apparent S.G.	S.G.	Solid phase	Total pore	Active pore	Semi-active pore	Dead pore	Semi-dead pore	Secondary pore
4.8 -9.52	Pumice	0.57	2.32	24.57	75.43	20.83	33.59	9.77	9.85	1.38
2.0 -4.8	Pumice	0.64	2.32	27.59	72.41	31.91	20.00	11.43	7.70	1.37
0.84-2.0	Pumice	0.73	2.34	31.20	68.80	37.61	14.28	11.49	3.51	1.91
0.42-0.84	mixture		2.53							
0.25-0.42	mixture		2.62							
<0.25	mixture		2.52							

is about 4:6 for 4.8–9.52 mm pumice, but 8:2 for lithic fragment and in case of the latter, the volume of both the total and the active pores increase to the distances. However, it is not clear in the inclination on the pore of the lithic fragment of Mt. Usu-c-Tephra at the plot in the long distance from the volcano, because this Tephra contain very less lithic fragment.

For the Usu-c-Tephra layer, the ratio of the real solid phase volume to the total pore volume is about 3:7 in average for pumice, but it is rather difficult to find a clear difference like in the Tarumai-b-Tephra layer. However the semi-dead pore volume is very large and the active pore volume is very small in the Usu-c-Tephra layer than in the Tarumai-b-Tephra layer. This fact points that the Usu-c-Tephra layer contains pores which are not concerned with the water holding capacity in high rate.

Beside the pores in pumices and in the lithic fragments, there is much space between pumice particles, and between pumice and/or many kinds of fragmenal particles; the authors calculated these void and the pore in a given volume of each Tephra layer. The data are shown in Fig. 4A to Fig. 4J. The samples which are taken the given volume (1000 cc) for a pipe core were shieved in nine fractions, and each fraction is separated in some mineralogical fractions. The apparent volume of each fraction is determined by paraffine method, and yet the apparent volume for smaller particles than 0.84 mm is determined in measuring syylinder, and the volume of space which lies between the mass of small particles is calculated for particles taking the

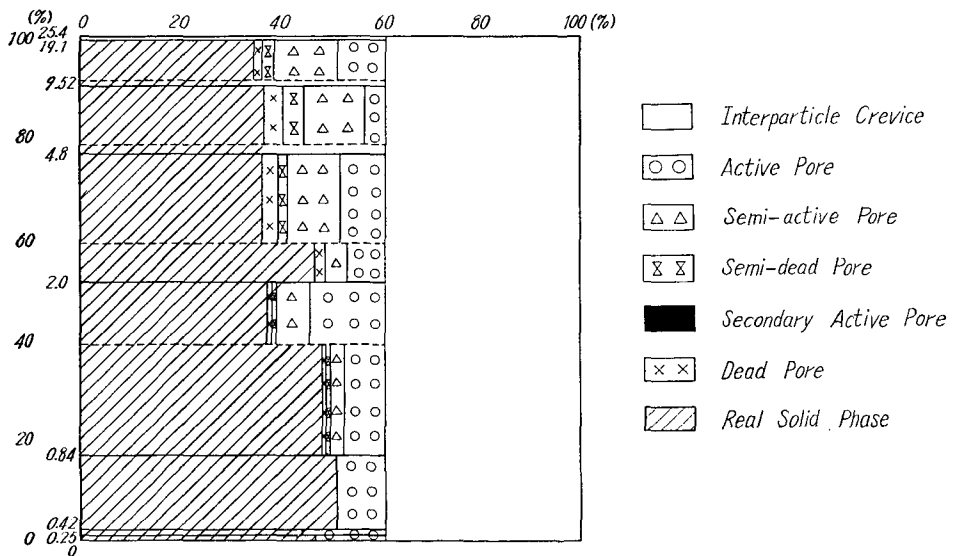


Fig. 4A. The Pore Distribution of Ta-b-Tomakomai-C₁ Tephra.

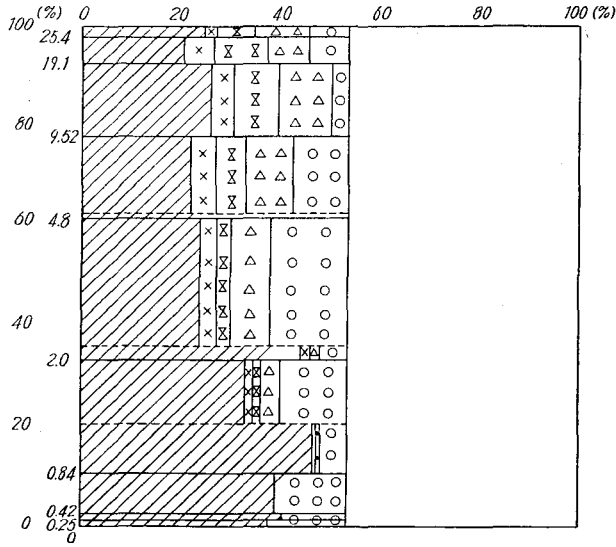


Fig. 4-B. The Pore Distribution of Ta-b-Tomakomai-C₂ Tephra.

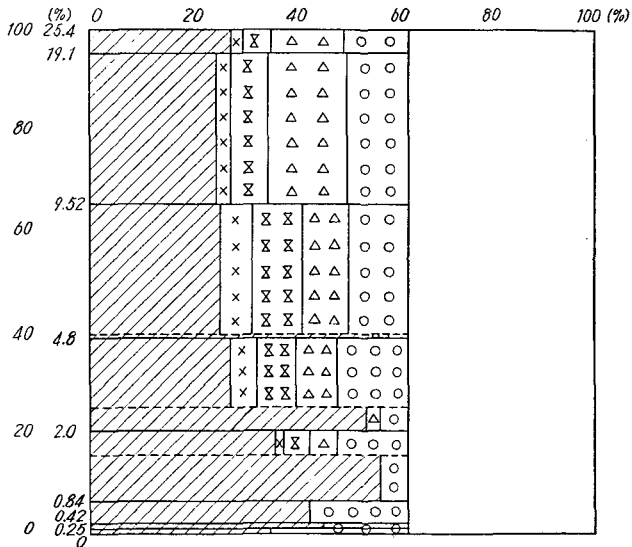


Fig. 4-C. The Pore Distribution of Ta-b-Tomakomai-C₂₋₂ Tephra.

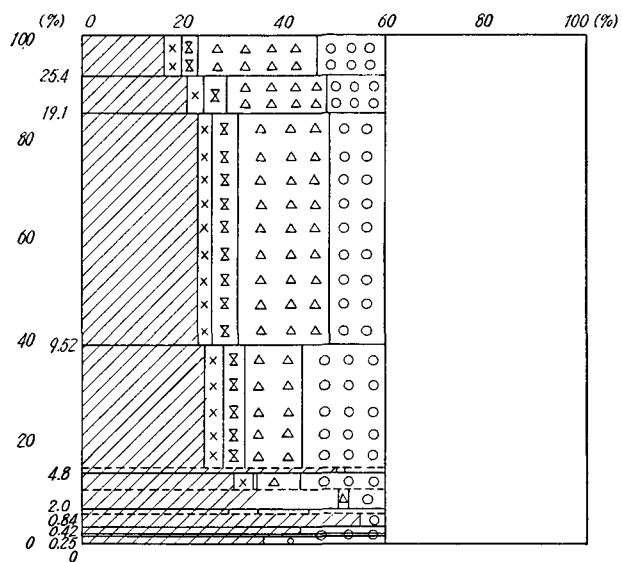


Fig. 4-D. The Pore Distribution of Ta-b-Tomakomai-C₃ Tephra.

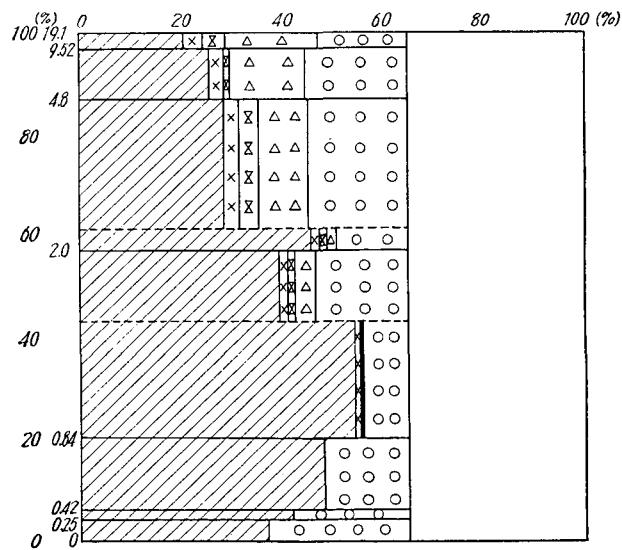


Fig. 4-E. The Pore Distribution of Ta-b-Fureoi-C₁ Tephra.

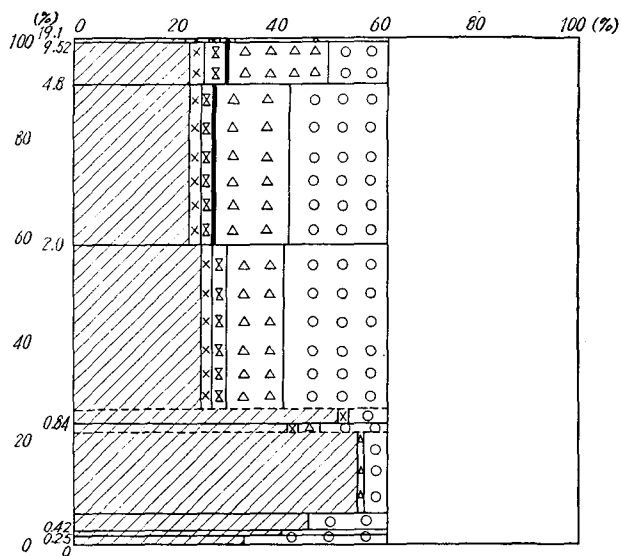


Fig. 4-F. The Pore Distribution of Ta-b-Fureoi-C₂ Tephra.

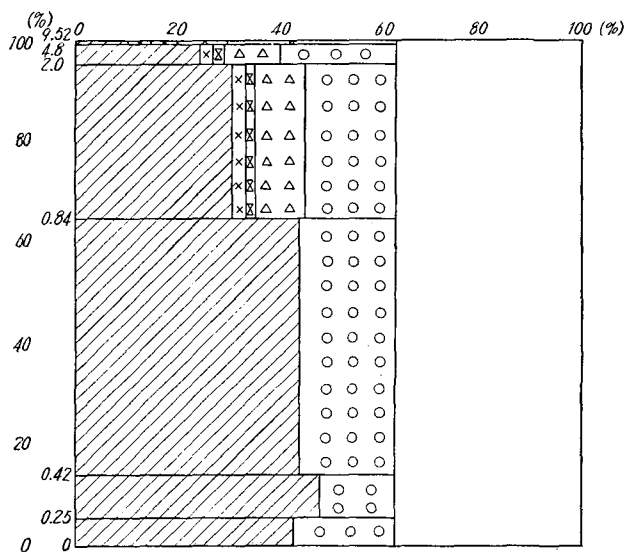


Fig. 4-G. The Pore Distribution of Ta-b-Hiraga-C Tephra.

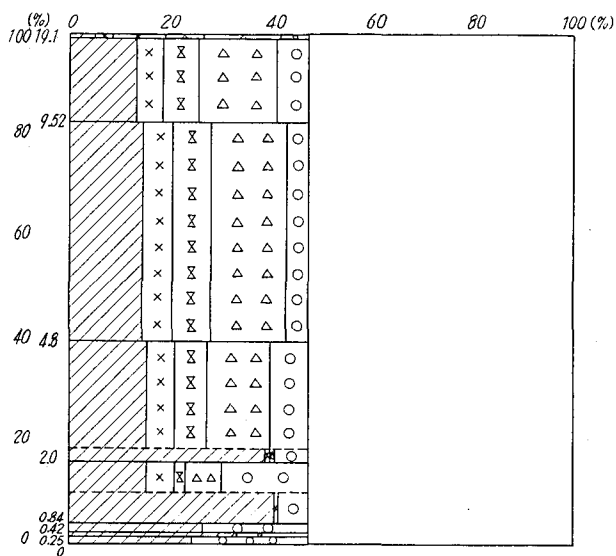


Fig. 4-H. The Pore Distribution of Us-c-Shadai-C1 Tephra.

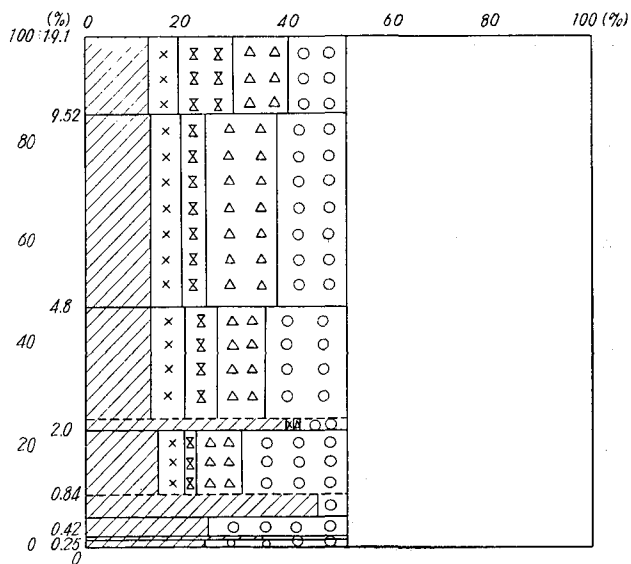


Fig. 4-I. The Pore Distribution of Us-c-Shadai-C2 Tephra.

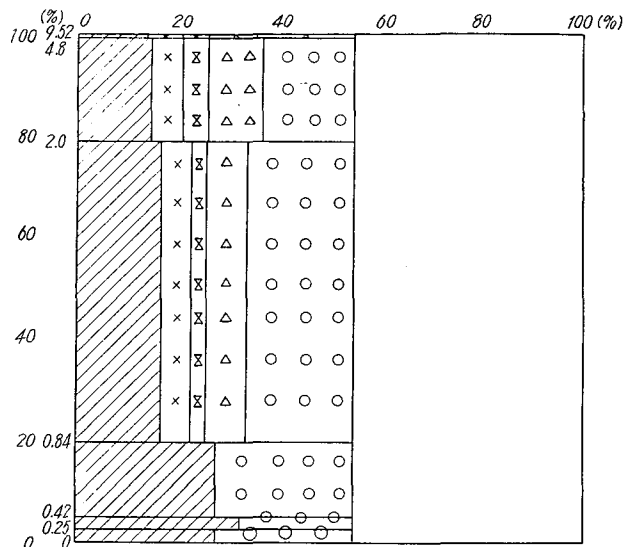


Fig. 4-J. The Pore Distribution of Us-c-Tomikawa-C Tephra.

TABLE 4. The Pore and Void Volume in Tephra Layer in Field Condition

	Tomakomai				Fureoi		Hiraga	Shadai		Niina
	C ₁	C ₂	C ₂₋₂	C ₃	C ₁	C ₂	C	C ₁	C ₂	C
Apparent void	39.3	47.1	36.9	40.2	34.9	38.5	36.7	52.7	51.3	45.2
Apparent solid phase	60.7	52.9	63.1	59.8	65.1	61.5	63.3	47.3	48.7	54.8
Real solid phase	42.6	29.1	31.1	25.1	39.6	30.8	39.8	17.4	16.2	18.3
Pore in particle	18.1	23.8	32.0	34.7	25.5	30.7	23.5	29.9	32.5	36.5
Active pore	8.6	10.2	12.3	11.2	16.2	15.3	18.0	6.8	14.5	20.7
Semi-active pore	6.1	6.5	9.6	15.5	5.8	11.3	3.4	12.4	8.0	7.8
Dead pore	1.8	3.0	3.7	3.2	1.7	1.9	1.2	4.6	4.9	5.2
Semi-dead pore	1.4	3.9	6.0	4.5	1.6	2.0	0.8	5.8	4.8	2.5
Secondary pore	0.2	0.2	0.4	0.3	0.2	0.2	0.1	0.2	0.3	0.3

intermediate state of hexahedral and octahedral configuration. Thus, the apparent particle volumes of this small size fraction is calculated from this particle volume (63.2%). The percent of the apparent volume of each size fraction to the sum of apparent volumes is calculated, then, they could get the interparticle space volume from the total apparent volume and the volume

of the sampling pipe cores.

From the above-mentioned data, they could estimate the following order on the each volume of the Tephra constituents, the space, and/or the pore: for solid phase volume of Tarumai-Tephra layer except Hokkaido Univ. Forest-C₁-Tephra;

Hiraga > Fureoi > Hokkaido Univ. Forest

for the space volume between particles;

Hokkaido Univ. Forest > Fureoi > Hiraga

and for the pore volume of ejectas (especially for pumice):

Hokkaido Univ. Forest > Fureoi > Hiraga.

In the case of Usu-Tephra, the solid phase volume is larger in Shadai sample than Niina's. For the space volume inter-particles, Shadai > Niina, and for the pore volume of ejectas, Shadai < Niina.

Summary

1. The authors developed the method to determine the pore space volume which was classified in five types.

2. The five types of pores of pumice or other pyroclastic ejectas were active, semi-active, secondary active, semi-dead, and dead pores.

3. The relation between the distribution and the ratio of these pores of ejectas and the distances from craters were investigated for Tarumai-b-Tephra layer and Usu-c-Tephra layer.

4. In this report mainly the Terumai-b-Tephra layer was discussed, and other Tephra layer shows the similar inclination.

5. The total pore volume of pumice became larger according to the distances from craters.

6. The material having larger total pore volumes are large in the pore volume, but the semi-active pore volume of ejecta became smaller by the distance, and the non-active pore volume had no relation to the distance.

7. The authors showed all the pore space volumes of Tephra layer had the similar inclinations to these of pumices, because these Tephra layers were made by principally pumices.

Reference

- 1) T. MAEDA, S. SASAKI and T. SASAKI: 1970. Studies on Physical Properties of Volcanic Soils in Hokkaido. II Properties of Pumice with Respect to Water. Trans. JSIDRE. 31, 25.
- 2) S. SASAKI: 1957. The Genetic Studies on Volcanic Ash Soil I. Sci. Soil and Manure, Japan 28, 59.

- 3) G. A. BORCHARDT, A. A. THEISEN, and M. E. HARWARD: 1968. Vesicular Pores of Pumice by Mercury Intrusion. Soil Sci. Soc. Am. Proc. 32, 735.
- 4) T. SASAKI, T. MAEDA, and S. SASAKI: 1969. Studies on Physical Properties of Volcanic Soils in Hokkaido, Japan. I. Pores of Pumices. Trans. JSIDRE. 27, 57.